Research Repository UCD

Title	A mathematical model for elasticity using calculus on discrete manifolds
Authors(s)	Dassios, Ioannis K., O'Keeffe, Gary, Jivkov, Andrey P.
Publication date	2018-04-27
Publication information	Dassios, Ioannis K., Gary O'Keeffe, and Andrey P. Jivkov. "A Mathematical Model for Elasticity Using Calculus on Discrete Manifolds." Wiley Online Library, April 27, 2018. https://doi.org/10.1002/mma.4892.
Publisher	Wiley Online Library
Item record/more information	http://hdl.handle.net/10197/10636
Publisher's statement	This is the peer reviewed version of the following article: Dassios, I, O'Keeffe, G, Jivkov, AP. A mathematical model for elasticity using calculus on discrete manifolds. Mathematical Methods in Applied Sciences. 2018; 41: 9057– 9070. https://doi.org/10.1002/mma.4892. This article may be used for non-commercial purposes in accordance with Wiley Terms and Conditions for Self-Archiving.
Publisher's version (DOI)	10.1002/mma.4892

Downloaded 2026-05-02 00:27:52

The UCD community has made this article openly available. Please share how this access benefits you. Your story matters! (@ucd_oa)

© Some rights reserved. For more information

Received <day> <Month>, <year>; | Revised <day> <Month>, <year>; | Accepted <day> <Month>, <year>

DOI: xxx/xxxx

ARTICLE TYPE

A mathematical model for elasticity using calculus on discrete manifolds

Ioannis Dassios*[1] | Gary O' Keeffe[2] | Andrey P Jivkov[3]

[1]ESIPP, University College Dublin, Ireland
[2]MACSI, Department of Mathematics & Statistics, University of Limerick, Ireland
[3]Mechanics of Physics of Solids Research Group, School of Mechanical Aerospace & Civil Engineering, The University of Manchester, UK

Correspondence
*Ioannis Dassios Email: ioannis.dassios@ucd.ie

Abstract

We propose a mathematical model to represent solid materials with discrete lattices and to analyse their behaviour by calculus on discrete manifolds. Focus is given on the mathematical derivation of the lattice elements by taking into account the stored energy associated with them. We provide a matrix formulation of the non-linear system describing elasticity with exact kinematics, known as finite strain elasticity in continuum mechanics. This formulation is ready for software implementation, and may also be used in atomic scale models as an alternative to existing empirical approach with pair and cohesive potentials. An illustrative example, analysing a local region of a node, is given to demonstrate the model performance.

KEYWORDS:
discrete manifold, lattice model, steel microstructure, elasticity, energy, non-linear system

1 | INTRODUCTION

Lattice models for deformation and fracture of solid materials were developed firstly for quasi-brittle materials, such as concretes and rocks (1), (7), and extended recently for elastic-plastic materials, such as structural steels (2). The benefit of modelling materials, treated as continua in classical mechanics, with discrete lattices is that the nucleation, growth and coalescence of discontinuities (cracks) become natural processes. As these are non-topological changes in the system, the classical solid mechanics, being a thermodynamic *bulk* theory, does not work. Additional benefit of the discrete approach is the possibility for introducing heterogeneities and local anisotropies in the modelled structure by appropriate spatial and directional variation of lattice properties, as well as natural and/or essential boundary conditions in what would be considered an interior in the continuum approach (since each lattice vertex is a boundary).

A lattice, in the language of algebraic topology, is a 1-complex embedded in $\mathbb{R}^2$ or $\mathbb{R}^3$, i.e. a graph with nodes (sites) equipped with Cartesian coordinates and edges (bonds) between some nodes. The first challenge is to ensure the elastic response of a graph is equivalent to the *continuum* response measured experimentally, i.e. to derive a link between properties of lattice elements, e.g. bond stiffness coefficients, and macroscopic properties. Isotropic materials, described by two macroscopic constants, can be represented exactly by $2D$ graphs based on hexagonal structure, e.g. (3), (5), (9), and by $3D$ graphs based on truncated octahedral structure (8), (12). Other regular $3D$ graphs can represent cubic elasticity, described by three macroscopic constants (10). However, there is no general recipe for deriving properties of lattice elements of arbitrary non-regular graph, which is required to represent closely given material microstructure, and all the existing representations with regular lattices are derived for linearised kinematics (infinitesimal strain in continuum settings). One of the aims of this work is to develop an alternative description of lattice behaviour, which makes arbitrary graphs represent macroscopic elasticity with exact kinematics (finite strain in continuum settings).

A mathematically rigorous analysis of graphs is based on discrete exterior calculus (DEC) (6). However, the analysis on graphs developed in this reference is applicable to physical problems, where the nodal unknown (a 0-cochain) is a scalar, i.e. temperature, pressure, concentration, etc, and its gradient is also a scalar over the edges (1-cochain). In mechanical problems the nodal unknown is a vector, e.g. nodal displacements in linearised kinematics or nodal coordinates in exact kinematics, which makes the problem critically different. One possibility for formulating elasticity is to use 3-complexes (11), which leads to a complexity similar to the one discretising continuum problems with finite elements for example. The main aim of this work is to investigate whether 1-complexes can still be used to describe elastic behaviour as computationally more efficient alternative to 3-complexes.

2 | THE MODEL WITH CALCULUS ON DISCRETE MANIFOLDS

Consider a tessellation of a 3D region into cells, e.g. a Voronoi tessellation around a given set of N points, representing a particular material microstructure (2). The tessellation is a 3-complex denoted by V and containing N 3-cells (cells), N_2 2-cells (faces), N_1 1-cells (edges) and N_0 0-cells (nodes). We explore the possibility to replace V with two 1-complexes (graphs), basic and complimentary, determined by V. The basic graph, denoted by G, has $n = N$ nodes placed at 3-cells' centres, and $m = N2$ edges connecting nodes whose 3-cells have common 2-cells. The connectivity of G is thus provided by the cell-face connectivity of V. The complementary graph, denoted by G* has $n^* = m = N_2$ nodes, placed at 2-cells's centres (which are also centres of G edges), $m^* = N_1$ edges connecting nodes whose 2-cells have common 1-cells. The connectivity of G* is thus provided by the face-edge connectivity of V.

To describe operations on G we introduce a matrix $A = [a_{ij}]_{i=1,2,...,m}^{j=1,2,...,n} \in \mathbb{R}^{m\times n}$, and a matrix $S = [s_{ij}]_{i=1,2,...,m}^{j=1,2,...,n} \in \mathbb{R}^{m\times n}$, where

$$a_{ij} = \left\{ \begin{array}{l} 0, \quad \text{if node } j \text{ is not a node of edge } i \\ 1, \quad \text{if node } j \text{ is the first node of edge } i \\ -1, \text{ if node } j \text{ is the second node of edge } i \end{array} \right\} \quad \text{and} \quad s_{ij} = \left\{ \begin{array}{l} 0, \quad \text{if node } j \text{ is not a node of edge } i \\ 0.5, \quad \text{if node } j \text{ is a node of edge } i \end{array} \right\}.$$

These reflect the cell-face connectivity of V: A is the standard incidence matrix, providing a co-boundary operator for nodes (6), while S is an averaging operator over nodes. Similar operators can be defined for G*, of which we will need only the co-boundary operator $A^* = [a^*_{ij}]_{i=1,2,...,m^*}^{j=1,2,...,n^*} \in \mathbb{R}^{m^*\times n^*}$ constructed similarly to A but reflecting face-edge connectivity of V.

Let

$$C = \begin{bmatrix} C_1 \\ C_2 \\ \vdots \\ C_n \end{bmatrix} \in \mathbb{R}^{n\times 3} \quad \text{and} \quad C^* = \begin{bmatrix} C^*_1 \\ C^*_2 \\ \vdots \\ C^*_n \end{bmatrix} \in \mathbb{R}^{n^*\times 3}$$

denote discrete vector-valued functions over nodes of G and G*, respectively, where

$$C_j = \begin{bmatrix} C_{j1} & C_{j2} & C_{j3} \end{bmatrix} \in \mathbb{R}^3, \quad j = 1, 2, ..., n \quad \text{and} \quad C^*_j = \begin{bmatrix} C^*_{j1} & C^*_{j2} & C^*_{j3} \end{bmatrix} \in \mathbb{R}^3, \quad j = 1, 2, ..., n^*.$$

In order to apply A, S and A^* on such functions we expand these operators by repetition of each raw and each column three times, so that from now on we will use the resultant $A \in \mathbb{R}^{3m\times 3n}$, $S \in \mathbb{R}^{3m\times 3n}$ and $A^* \in \mathbb{R}^{3m^*\times 3n^*}$. When A and A^* are applied to C and C^* they provide the gradient of these functions as vector-valued functions over edges of the respective graphs

$$AC = b = \begin{bmatrix} b_1 \\ b_2 \\ \vdots \\ b_m \end{bmatrix} \in \mathbb{R}^{m\times 3} \quad \text{and} \quad A^*C^* = b^* = \begin{bmatrix} b^*_1 \\ b^*_2 \\ \vdots \\ b^*_m \end{bmatrix} \in \mathbb{R}^{m^*\times 3}$$

where

$$b_i = \begin{bmatrix} b_{i1} & b_{i2} & b_{i3} \end{bmatrix} \in \mathbb{R}^3, \quad i = 1, 2, ..., m \quad \text{and} \quad b^*_i = \begin{bmatrix} b^*_{i1} & b^*_{i2} & b^*_{i3} \end{bmatrix} \in \mathbb{R}^3, \quad i = 1, 2, ..., m^*.$$

For the purposes of developing exact kinematics, we associate C and C^* with the nodal coordinates in G and G*, respectively, in which case we note that $C^* = SC$. Further b and b^* represent coordinate differences associated with edges of G and G*, respectively, which provide edge lengths via $|b_i|$, $i = 1, 2, ..., m$, and $|b^*_i|$, $i = 1, 2, ..., m^*$.

A boundary value problem is formulated by prescribing boundary conditions to the nodes of G. These can be either natural, i.e. prescribed external forces, or essential, i.e. prescribed new coordinates due to nodal displacements. As a result of these

conditions, the geometry of the whole structure changes, so that the nodes of G and G* have new coordinates

$$X_j = \begin{bmatrix} X_{j1} & X_{j2} & j3 \end{bmatrix} \in \mathbb{R}^3, \quad j = 1, 2, ..., n \quad \text{and} \quad X_j^* = \begin{bmatrix} X_{j1}^* & X_{j2}^* & X_{j3}^* \end{bmatrix} \in \mathbb{R}^3, \quad j = 1, 2, ..., n^*,$$

which we assume to be related by $X^* = SX$, i.e. the deformation of G* is *induced* by the deformation of G. This leads to new edge lengths calculated as $|y_i|$, $i = 1, 2, ..., m$, and $|y_i^*|$, $i = 1, 2, ..., m^*$ from

$$y = AX = \begin{bmatrix} y_1 \\ y_2 \\ \vdots \\ y_m \end{bmatrix} \in \mathbb{R}^{m\times 3} \quad \text{and} \quad y^* = A^*X^* = A^*SX = \begin{bmatrix} y_1^* \\ y_2^* \\ \vdots \\ y_{m^*}^* \end{bmatrix} \in \mathbb{R}^{m^*\times 3}. \tag{1}$$

Upon deformation, the edges of G and G* store elastic energy dependent on the length changes $|y_i| - |b_i|$, $i = 1, 2, ..., m$ and $|y_i^*| - |b_i^*|$, $i = 1, 2, ..., m^*$, respectively. As a first approximation, we assume the edge energies to be quadratic functions of length changes within specified length intervals as follows

$$U_i = K_i(|y_i| - |b_i|)^2, \quad a_{0i} \le |y_i| - |b_i| \le a_{1i}, \quad i = 1, 2, ..., m \quad \text{and} \tag{2}$$

$$U_i^* = K_i^*(|y_i^*| - |b_i^*|)^2, \quad a_{2i} \le |y_i^*| - |b_i^*| \le a_{3i}, \quad i = 1, 2, ..., m^*, \tag{3}$$

where K_i and K_i^* are material parameters associated with the edges of G and G*, respectively, and the intervals $[a_{0i}, a_{1i}]$ and $[a_{2i}, a_{3i}]$ provide the limits for local physically linear behaviour. Taking into account that the deformation of G* is induced by $X^* = SX$, it is clear that the system unknowns (nodal coordinates) are associated with the nodes of G only and correspondingly the system reaction (edge forces) need to be associated with the edges of G only. To achieve this, we associate the stored energy of the system only with the edges of G, making the total energy of G-edge i equal to the sum of its internal energy, U_i, and half of the energies in the G*-edges incident with the G*-node centred at G-edge i. This can be written as $\frac{1}{2}\sum_k U_k^*$, where the sum is over the G*-edges incident with the G*-node. Thus, the total stored energy associated with each edge of G is given by

$$W_i = U_i + \frac{1}{2}\sum_k U_k^*, \quad i = 1, 2, ..., m. \tag{4}$$

The gradient of the total energy with respect to the change of edge length, provides the magnitude of the force in the G-edge, i.e. for $|y_i| \neq |b_i|$ we have

$$|F_i| = \frac{W_i}{|y_i| - |b_i|}, \quad i = 1, 2, ..., m. \tag{5}$$

Finally, we restrict our present consideration to materials with non-polar behaviour by constraining the forces in G-edges to act along the edges in the deformed state, i.e. $F_i || y_i$, $i = 1, 2, ..., m$. Hence, if $T_i = \frac{y_i}{|y_i|}$, $i = 1, 2, ..., m$ are the unit vectors along edges in G, the edge forces are calculated by

$$F_i = |F_i|T_i = \frac{|F_i|}{|y_i|}y_i, \quad i = 1, 2, ..., m. \tag{6}$$

This can be summarised for the whole G by

$$F = g(|y|)y, \quad \text{where} \quad g(|y|) = diag\left\{\frac{|F_1|}{|y_1|}, \frac{|F_2|}{|y_2|}, \dots \frac{|F_m|}{|y_m|}\right\} \in \mathbb{R}^{m\times m}. \tag{7}$$

Let $B_i = \begin{bmatrix} B_{i1} & B_{i2} & B_{i3} \end{bmatrix} \in \mathbb{R}^3$, $i = 1, 2, ..., n$, be the external forces at the nodes of G, either provided as natural boundary conditions, or arising as reactions to essential boundary conditions. Since the balance of angular momentum is automatically fulfilled at all nodes by $F_i || y_i$, the equilibrium of the system with the boundary conditions is ensured by the balance of linear momentum at all nodes. This is given by

$$A^T F = B, \tag{8}$$

where $A^T \in \mathbb{R}^{n\times m}$ is the transpose of the incidence matrix A, a boundary operator on edges of G. By substituting (7) into (8), we get

$$A^T g(|y|)y = B, \tag{9}$$

which incorporates the contribution of G* to the equilibrium via (4) and (5)). By substituting (1) into (9), we arrive at the general description of the system elasticity in terms of positions and forces of nodes in G

$$[A^T g(|AX|)A]X = B. \tag{10}$$

The application of boundary conditions to the system (10) requires a separation of the nodal coordinate directions into two groups: directions with prescribed natural condition - a force component, which maybe zero (free boundary), and directions with prescribed essential condition - a new coordinate value which also maybe zero (fixed boundary). This separation can be represented by the following expressions for nodal positions and forces, and a correspondingly re-arranged incidence matrix

$$X = \begin{bmatrix} X^P \\ X^Q \end{bmatrix} \in \mathbb{R}^{n\times 3} \quad , \quad B = \begin{bmatrix} B^P \\ B^Q \end{bmatrix} \in \mathbb{R}^{n\times 3} \quad \text{and} \quad A = \begin{bmatrix} A^P \\ A^Q \end{bmatrix} \in \mathbb{R}^{3m\times 3n},$$

where $X^P \in \mathbb{R}^p$ and $B^P \in \mathbb{R}^p$ are vectors of the unknown coordinates and the known corresponding forces, $X^Q \in \mathbb{R}^q$ and $B^Q \in \mathbb{R}^q$ are vectors of the known coordinates and the unknown corresponding forces, and $p + q = 3n$ holds.

3 | MAIN RESULTS

System (10) is a non-linear system. This is because of the diagonal matrix $g(|AX|)$ defined in (8). We provide the following Theorem:

Theorem 1. *Consider the non-linear system* (10)*. Then*

(a) An effective linearization of the system is given by

$$\tilde{A}X = B. \tag{11}$$

Where $\tilde{A} = A^T\tilde{K}A$ *with* $\tilde{K} = diag[\tilde{K}_i]_{1\le i\le m}$ *and for* $0 < \epsilon << 1$

$$\tilde{K}_i = \begin{Bmatrix} K_i + \frac{1}{2}\sum_{z=0}^{1}\left[\frac{\sum_{j=1}^{m^*}[K_i^* a_{(z+2)i}^2]}{2a_{(1-z)i}(a_{(1-z)i}+|b_i|)} - \frac{K_i|b_i|}{a_{zi}+|b_i|}\right], & a_{0i} > 0, \quad a_{2i} \ge 0 \\ K_i + \frac{1}{2}\sum_{z=0}^{1}\left[\frac{\sum_{j=1}^{m^*}[K_i^* a_{(z+2)i}^2]}{a_{(1-z)i}(a_{0i}+a_{1i})} - \frac{K_i|b_i|}{a_{zi}+|b_i|}\right], & a_{0i} > 0, \quad a_{2i} \le 0 \\ K_i + \frac{1}{2}\sum_{z=0}^{1}\left[z\frac{\sum_{j=1}^{m^*}[K_i^* a_{(z+2)i}^2]}{2a_{(1-z)i}(a_{(1-z)i}+|b_i|)} - \frac{K_i|b_i|}{a_{zi}+|b_i|}\right], & a_{0i} < 0, \quad a_{2i} \ge 0 \\ K_i + \frac{1}{2}\sum_{z=0}^{1}\left[z\frac{\sum_{j=1}^{m^*}[K_i^* a_{(z+2)i}^2]}{a_{(1-z)i}(a_{0i}+a_{1i})} - \frac{K_i|b_i|}{a_{zi}+|b_i|}\right], & a_{0i} < 0, \quad a_{2i} \le 0 \end{Bmatrix}.$$

For $|y_i| = |b_i|$*, i.e.* $a_{0i} = 0$ *or* $a_{1i} = 0$*, we have* $\tilde{K}_i = \frac{|F_i|}{|b_i|}$.

(b) Let

$$\tilde{A} = \begin{bmatrix} \tilde{A}_{11} & \tilde{A}_{12} \\ \tilde{A}_{21} & \tilde{A}_{22} \end{bmatrix}.$$

Where $\tilde{A}_{11} \in \mathbb{R}^{p\times p}, \tilde{A}_{12} \in \mathbb{R}^{p\times q}, \tilde{A}_{21} \in \mathbb{R}^{q\times q}, \tilde{A}_{22} \in \mathbb{R}^{q\times q}$*. Then system* (11) *can be divided into the following subsystems*

$$\tilde{A}_{11}X^P = B^P - \tilde{A}_{12}X^Q \tag{12}$$

and

$$B^Q = \tilde{A}_{13}X^P + \tilde{A}_{22}X^Q. \tag{13}$$

From the above systems only (12) *has to be solved. Then* X^P *can be replaced in* (13) *and* B^Q *is easily computed.*

Proof. For the proof of (a) we consider (8)*,* (10) *and will seek optimal bounds for* $\frac{|F_i|}{|y_i|}$, $\forall i = 1, 2, ..., m$*. From* (5)

$$|F_i| = \frac{W_i}{|y_i| - |b_i|}, \quad i = 1, 2, ..., m,$$

whereby replacing (4) *into the above expression we get*

$$|F_i| = \frac{U_i + \frac{1}{2}\sum_{j=1}^{m^*} U_j^*}{|y_i| - |b_i|}, \quad i = 1, 2, ..., m.$$

By using (2) *and* (3) *we have*

$$|F_i| = \frac{K_i(|y_i| - |b_i|)^2 + \frac{1}{2}\sum_{j=1}^{m^*}[K_i^*(|y_i^*| - |b_i^*|)^2]}{|y_i| - |b_i|}, \quad i = 1, 2, ..., m,$$

or, equivalently,

$$|F_i| = K_i(|y_i| - |b_i|) + \frac{1}{2}\frac{\sum_{j=1}^{m^*}[K_i^*(|y_i^*| - |b_i^*|)^2]}{|y_i| - |b_i|}, \quad i = 1, 2, ..., m,$$

or, equivalently,

$$\frac{|F_i|}{|y_i|} = K_i(1 - \frac{|b_i|}{|y_i|}) + \frac{1}{2}\frac{\sum_{j=1}^{m^*}[K_i^*(|y_i^*| - |b_i^*|)^2]}{|y_i|(|y_i| - |b_i|)}, \quad i = 1, 2, ..., m. \tag{14}$$

From (2) *and* (3) *we have that*

$$a_{0i} \leq |y_i| - |b_i| \leq a_{1i}, \quad i = 1, 2, ..., m \quad and \quad a_{2i} \leq |y_i^*| - |b_i^*| \leq a_{3i}, \quad i = 1, 2, ..., m^*.$$

Hence we have

$$a_{2i}^2 \leq (|y_i^*| - |b_i^*|)^2 \leq a_{3i}^2, \quad if \quad a_{2i} \geq 0,$$

$$0 \leq (|y_i^*| - |b_i^*|)^2 \leq min\{a_{2i}^2, a_{3i}^2\}, \quad if \quad a_{2i} \leq 0,$$

or, equivalently, by multiplying the above expressions by K_i^*

$$K_i^* a_{2i}^2 \leq K_i^*(|y_i^*| - |b_i^*|)^2 \leq K_i^* a_{3i}^2, \quad if \quad a_{2i} \geq 0,$$

$$0 \leq K_i^*(|y_i^*| - |b_i^*|)^2 \leq K_i^* min\{a_{2i}^2, a_{3i}^2\}, \quad if \quad a_{2i} \leq 0.$$

or, equivalently, by summing

$$\begin{aligned} &\textstyle\sum_{j=1}^{m^*}[K_i^* a_{2i}^2] \leq \sum_{j=1}^{m^*}[K_i^*(|y_i^*| - |b_i^*|)^2] \leq \sum_{j=1}^{m^*}[K_i^* a_{3i}^2], \quad if \quad a_{2i} \geq 0, \\ &0 \leq \textstyle\sum_{j=1}^{m^*}[K_i^*(|y_i^*| - |b_i^*|)^2] \leq \sum_{j=1}^{m^*}[K_i^* min\{a_{2i}^2, a_{3i}^2\}], \quad if \quad a_{2i} \leq 0. \end{aligned} \tag{15}$$

Furthermore, we have

$$a_{0i} + |b_i| \leq |y_i| \leq a_{1i} + |b_i|,$$

or, equivalently,

$$\frac{a_{0i} + |b_i|}{|b_i|} \leq \frac{|y_i|}{|b_i|} \leq \frac{a_{1i} + |b_i|}{|b_i|},$$

or, equivalently,

$$\frac{|b_i|}{a_{1i} + |b_i|} \leq \frac{|b_i|}{|y_i|} \leq \frac{|b_i|}{a_{0i} + |b_i|},$$

or, equivalently,

$$1 - \frac{|b_i|}{a_{0i} + |b_i|} \leq 1 - \frac{|b_i|}{|y_i|} \leq 1 - \frac{|b_i|}{a_{1i} + |b_i|}.$$

or, equivalently,

$$K_i(1 - \frac{|b_i|}{a_{0i} + |b_i|}) \leq K_i(1 - \frac{|b_i|}{|y_i|}) \leq K_i(1 - \frac{|b_i|}{a_{1i} + |b_i|}). \tag{16}$$

Also from the above expressions

$$\frac{1}{a_{1i} + |b_i|} \leq \frac{1}{|y_i|} \leq \frac{1}{a_{0i} + |b_i|}. \tag{17}$$

Finally

$$\begin{aligned} &\tfrac{1}{a_{1i}} \leq \tfrac{1}{|y_i| - |b_i|} \leq \tfrac{1}{a_{0i}}, \quad if \quad a_{0i} > 0, \\ &\tfrac{1}{|y_i| - |b_i|} \cong \tfrac{2}{a_{0i} + a_{1i}} \pm \epsilon, \quad if \quad a_{0i} < 0. \end{aligned} \tag{18}$$

Hence, for $a_{0i} > 0$ *and* $a_{2i} \geq 0$, *from* (15), (16), (17) *and* (18), *we have*

$$K_i(1 - \frac{|b_i|}{a_{0i} + |b_i|}) + \frac{\sum_{j=1}^{m^*}[K_i^* a_{2i}^2]}{2a_{1i}(a_{1i} + |b_i|)} \leq \frac{|F_i|}{|y_i|} \leq K_i(1 - \frac{|b_i|}{a_{1i} + |b_i|}) + \frac{\sum_{j=1}^{m^*}[K_i^* a_{3i}^2]}{2a_{0i}(a_{0i} + |b_i|)},$$

or, equivalently,

$$\frac{|F_i|}{|y_i|} \cong K_i + \frac{1}{2}\sum_{z=0}^{1}\left[\frac{\sum_{j=1}^{m^*}[K_i^* a_{(z+2)i}^2]}{2a_{(1-z)i}(a_{(1-z)i} + |b_i|)} - \frac{K_i|b_i|}{a_{zi} + |b_i|}\right] \pm \epsilon, \quad i = 1, 2, ..., m.$$

For $a_{0i} > 0$ and $a_{2i} \leq 0$, from (15), (16), (17) *and* (18)*, we have*

$$K_i(1 - \frac{|b_i|}{a_{0i} + |b_i|}) + \frac{\sum_{j=1}^{m^*}[K_i^* a_{2i}^2]}{a_{1i}(a_{0i} + a_{1i})} \leq \frac{|F_i|}{|y_i|} \leq K_i(1 - \frac{|b_i|}{a_{1i} + |b_i|}) + \frac{\sum_{j=1}^{m^*}[K_i^* a_{3i}^2]}{a_{0i}(a_{0i} + a_{1i})},$$

or, equivalently,

$$\frac{|F_i|}{|y_i|} \cong K_i + \frac{1}{2}\sum_{z=0}^{1}\left[\frac{\sum_{j=1}^{m^*}[K_i^* a_{(z+2)i}^2]}{a_{(1-z)i}(a_{0i} + a_{1i})} - \frac{K_i|b_i|}{a_{zi} + |b_i|}\right] \pm \epsilon, \quad i = 1, 2, ..., m.$$

For $a_{0i} < 0$ and $a_{2i} \geq 0$, we have

$$K_i(1 - \frac{|b_i|}{a_{0i} + |b_i|}) \leq \frac{|F_i|}{|y_i|} \leq K_i(1 - \frac{|b_i|}{a_{1i} + |b_i|}) + \frac{\sum_{j=1}^{m^*}[K_i^* a_{3i}^2]}{2a_{0i}(a_{0i} + |b_i|)},$$

or, equivalently,

$$\frac{|F_i|}{|y_i|} \cong K_i + \frac{1}{2}\sum_{z=0}^{1}\left[z\frac{\sum_{j=1}^{m^*}[K_i^* a_{(z+2)i}^2]}{2a_{(1-z)i}(a_{(1-z)i} + |b_i|)} - \frac{K_i|b_i|}{a_{zi} + |b_i|}\right] \pm \epsilon, \quad i = 1, 2, ..., m.$$

For $a_{0i} < 0$ and $a_{2i} \leq 0$, we have

$$K_i(1 - \frac{|b_i|}{a_{0i} + |b_i|}) \leq \frac{|F_i|}{|y_i|} \leq K_i(1 - \frac{|b_i|}{a_{1i} + |b_i|}) + \frac{\sum_{j=1}^{m^*}[K_i^* a_{3i}^2]}{a_{0i}(a_{0i} + a_{1i})},$$

or, equivalently,

$$\frac{|F_i|}{|y_i|} \cong K_i + \frac{1}{2}\sum_{z=0}^{1}\left[z\frac{\sum_{j=1}^{m^*}[K_i^* a_{(z+2)i}^2]}{a_{(1-z)i}(a_{0i} + a_{1i})} - \frac{K_i|b_i|}{a_{zi} + |b_i|}\right] \pm \epsilon, \quad i = 1, 2, ..., m.$$

It is easy to observe that for $|y_i| = |b_i|$, i.e. $a_{0i} = 0$ or $a_{1i} = 0$, and from (8) *we have $\tilde{K}_i = \frac{|F_i|}{|b_i|}$. The proof of (b) is trivial and a similar one can be found in (2). The proof is completed.* □

For an alternative numerical method with iterations to solve the non-linear system (10), we provide the following Theorem.

Theorem 2. *An iterative method for solving the non-linear system* (10) *is*

$$G_k X_{k+1} = B_{k+1}. \tag{19}$$

Where

$$X_k = \begin{bmatrix} X_k^P \\ X^Q \end{bmatrix}, \quad B_k = \begin{bmatrix} B^P \\ B_k^Q \end{bmatrix}.$$

$$G_k = A^T g(|y_{i,k}|)A$$

and

$$g(|y_{i,0}|) = diag\left[K_i(1 - \frac{2|b_i|}{2|b_i| + a_{0i} + a_{1i}}) + \frac{1}{2}\frac{\sum_{j=1}^{m^*}[K_i^*(a_{2i} + a_{3i})^2]}{(2|b_i| + a_{0i} + a_{1i})(a_{0i} + a_{1i})}\right]_{1 \leq i \leq m}.$$

Furthermore let

$$G_k = \begin{bmatrix} G_k^{11} & G_k^{12} \\ G_k^{21} & G_k^{22} \end{bmatrix};$$

Then, a solution of (10) *through a first iteration of* (19) *is given by*

$$\begin{gathered} X_1^P = (G_0^{(11)})^\dagger[B^P - G_0^{(12)}X^Q] \\ \text{and} \\ B_1^Q = G_0^{(21)}\left[(G_0^{(11)})^\dagger[B^P - G_0^{(12)}X^Q]\right] + G_0^{(22)}X^Q. \end{gathered} \tag{20}$$

If $G_0^{(11)}$ is invertible then $(G_0^{(11)})^\dagger$ is its inverse and when $G_0^{(11)}$ is singular then $(G_0^{(11)})^\dagger$ is its pseudoinverse.

Proof. We seek a method of solution for the non-linear system (10)

$$[A^T g(|AX|)A]X = B.$$

Based on the special structure of $A^T g(|AX|)A$ we may use the Picard method and construct the matrix difference equation

$$[A^T g(|AX_k|)A]X_{k+1} = B_{k+1}$$

or, equivalently, by replacing $y_{i,k} = AX_k$

$$[A^T g(|y_{i,k}|)A]X_{k+1} = B_{k+1},$$

or, equivalently, for $G_k = A^T g(|y_{i,k}|)A$ we arrive at (19)*. Note that*

$$X_k = \begin{bmatrix} X_k^P \\ X^Q \end{bmatrix}, \quad B_k = \begin{bmatrix} B^P \\ B_k^Q \end{bmatrix},$$

because X^Q, B^P are considered known while X^P, B^Q are unknown. Since $a_{0i} \leq |y_i| - |b_i| \leq a_{1i}$ for $i = 1, 2, ..., m$ and $a_{2i} \leq |y_i^*| - |b_i^*| \leq a_{3i}$ for $i = 1, 2, ..., m^*$, we may use $|y_{i,0}| = \frac{a_{0i}+a_{1i}-2|b_i|}{2}$ and $|y_{i,0}^*| = \frac{a_{2i}+a_{3i}-2|b_i^*|}{2}$ as an initial approximation. Then

$$G_0 = A^T g(|y_{i,0}|)A,$$

where

$$g(|y_{i,0}|) = diag\left\{\frac{|F_{i,k}|}{|y_{i,k}|}\right\}_{i=1,2,...,m}.$$

or, equivalently

$$g(|y_{i,0}|) = diag\left\{K_i(1 - \frac{|b_i|}{|y_i|}) + \frac{1}{2}\frac{\sum_{j=1}^{m^*}[K_i^*(|y_i^*| - |b_i^*|)^2]}{|y_i|(|y_i| - |b_i|)}\right\}_{i=1,2,...,m}.$$

or, equivalently

$$g(|y_{i,0}|) = diag\left\{K_i(1 - \frac{2|b_i|}{a_{0i} + a_{1i} - 2|b_i|}) + \frac{1}{2}\frac{\sum_{j=1}^{m^*}[K_i^*(a_{2i} + a_{3i} - 2|b_i^*|)^2]}{(a_{0i} + a_{1i} - 2|b_i|)(a_{0i} + a_{1i})}\right\}_{i=1,2,...,m}.$$

Hence for

$$G_0 = \begin{bmatrix} G_0^{11} & G_0^{12} \\ G_0^{21} & G_0^{22} \end{bmatrix},$$

a first iteration is given by

$$G_0 X_1 = B_1,$$

or, equivalently,

$$\begin{bmatrix} G_0^{11} & G_0^{12} \\ G_0^{21} & G_0^{22} \end{bmatrix} \begin{bmatrix} X_1^P \\ X^Q \end{bmatrix} = \begin{bmatrix} B^P \\ B_1^Q \end{bmatrix}.$$

or, equivalently,

$$G_0^{(11)} X_1^P + G_0^{(12)} X^Q = B^P$$

$$G_0^{(21)}\left[(G_0^{(11)})^\dagger [B^P - G_0^{(12)} X^Q]\right] + G_0^{(22)} X^Q = B_1^Q$$

and from here we arrive easily at (20)*. The proof is completed.* □

For the non-linear system (10), let

$$A^T g(|AX|)A = G(X) = \begin{bmatrix} G^{11}(X) & G^{12}(X) \\ G^{21}(X) & G^{22}(X) \end{bmatrix}.$$

Then for

$$X = \begin{bmatrix} X^P \\ X^Q \end{bmatrix}, \quad B = \begin{bmatrix} B^P \\ B^Q \end{bmatrix},$$

we have

$$X^P = (G^{(11)}(X))^\dagger [B^P - G^{(12)}(X)X^Q], \quad B^Q = G^{(21)}(X)\left[(G^{(11)}(X))^\dagger [B^P - G^{(12)}(X)X^Q]\right] + G^{(22)}(X)X^Q,$$

and consequently the iterative method (19) converges for

$$\left\|\nabla\left\{(G^{(11)}(X))^\dagger [B^P - G^{(12)}(X)X^Q]\right\}\right\| < 1, \quad \left\|\nabla\left\{G^{(21)}(X)\left[(G^{(11)}(X))^\dagger [B^P - G^{(12)}(X)X^Q]\right] + G^{(22)}(X)X^Q\right\}\right\| < 1.$$

With $\|\cdot\|$ we denote an induced norm. The numerical method (19) can be more efficient than the linearization in Theorem 1 if the above expressions hold, and only after many iterations. However, besides these restrictions, the method in Theorem 1 is more useful because it has low memory requirements and avoids matrix factorizations.

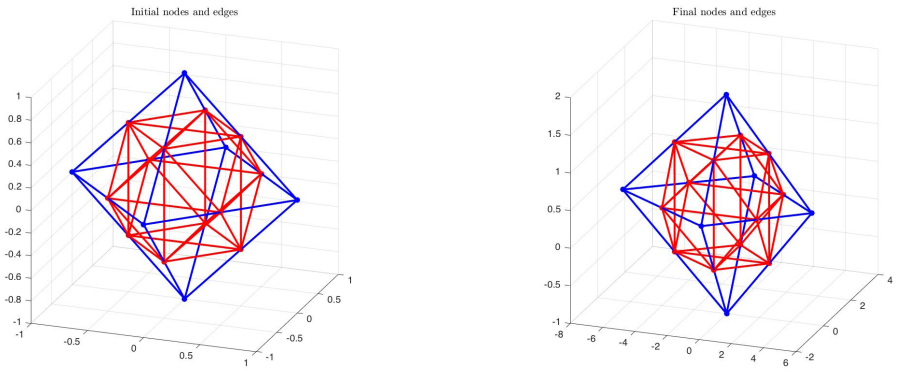

FIGURE 1 *Numerical Example: On the left the graph with the initial positions and edges and on the right the graph with the final positions and edges*

i	C_i	C_i^*	b_i	$\|b_i\|$	b_i^*	$\|b_i^*\|$
1	(0, 0,1)	(-0.5,0,0.5)	(1,0,1)	$\sqrt{2}$	(-0.5,-0.5,0)	$1/\sqrt{2}$
2	(1,0,0)	(0,0.5,0.5)	(0,-1,1)	$\sqrt{2}$	(-0.5,0.5,0)	$1/\sqrt{2}$
3	(0,-1,0)	(0.5,0,0.5)	(-1,0,1)	$\sqrt{2}$	(0.5,0.5,0)	$1/\sqrt{2}$
4	(-1,0,0)	(0,-0.5,0.5)	(0,1,1)	$\sqrt{2}$	(0.5,-0.5,0)	$1/\sqrt{2}$
5	(0,1,0)	(-0.5,-0.5,0)	(1,-1,0)	$\sqrt{2}$	(0,0.5,0.5)	$1/\sqrt{2}$
6	(0,0,-1)	(-0.5,0.5,0)	(-1,-1,0)	$\sqrt{2}$	(0,-0.5,0.5)	$1/\sqrt{2}$
7		(0.5,0.5,0)	(-1,1,0)	$\sqrt{2}$	(0.5,0,0.5)	$1/\sqrt{2}$
8		(0.5,-0.5,0)	(1,1,0)	$\sqrt{2}$	(-0.5,0,0.5)	$1/\sqrt{2}$
9		(-0.5,0,-0.5)	(1,0,-1)	$\sqrt{2}$	(0,-0.5,0.5)	$1/\sqrt{2}$
10		(0,0.5,-0.5)	(0,-1,-1)	$\sqrt{2}$	(0,0.5,0.5)	$1/\sqrt{2}$
11		(0.5,0,-0.5)	(-1,0,-1)	$\sqrt{2}$	(-0.5,0,0.5)	$1/\sqrt{2}$
12		(0,-0.5,-0.5)	(0,1,-1)	$\sqrt{2}$	(0.5,0,0.5)	$1/\sqrt{2}$
13					(0,-1,0)	1
14					(-1,0,0)	1
15					(0,1,0)	1
16					(1,0,0)	1
17					(-0.5,0,0.5)	$1/\sqrt{2}$
18					(0,-0.5,0.5)	$1/\sqrt{2}$
19					(0,0.5,0.5)	$1/\sqrt{2}$
20					(-0.5,0,0.5)	$1/\sqrt{2}$
21					(0.5,0,0.5)	$1/\sqrt{2}$
22					(0,0.5,0.5)	$1/\sqrt{2}$
23					(0,-0.5,0.5)	$1/\sqrt{2}$
24					(0.5,0,0.5)	$1/\sqrt{2}$
25					(-0.5,-0.5,0)	$1/\sqrt{2}$
26					(-0.5,0.5,0)	$1/\sqrt{2}$
27					(0.5,0.5,0)	$1/\sqrt{2}$
28					(0.5,-0.5,0)	$1/\sqrt{2}$
29					(-1,0,0)	1
30					(0,1,0)	1
31					(-1,0,0)	1
32					(0,1,0)	1
33					(0,0,1)	1
34					(0,0,1)	1
35					(0,0,1)	1
36					(0,0,1)	1

TABLE 1 *Initial nodes, edges, and edge lengths.*

Numerical example

Figure 1 illustrates a three-dimensional representation of the system modelled for demonstration purposes. In this example, we assume a lattice of a set of $n = 6$ nodes which are connected through $m = 12$ edges. A second set of $n^* = m = 12$ nodes are placed at the centres of the 12 primary edges and these secondary nodes are connected by $m^* = 36$ secondary edges. Table 1 provides coordinate values for nodes i.e., C_i, C_i^*, and vector values for edges, i.e., b_i, b_i^*. We then assume that a force F is applied to the primary edges. The forces, F_i, the material coefficients, i.e., K_i, K_i^*, and the bounds of (2) and (3), i.e., a_{0i}, a_{1i}, a_{3i}, a_{4i}, are given in Table 2. We solve the non-linear system (10) numerically by implementing the results of Theorem 1 in MATLAB, and this yields: the new coordinate values for the primary and secondary nodes, and vector values for the primary and secondary edges, i.e., X_i, X_i^*, and y_i, y_i^*, respectively (all of these values are provided in Table 3).

The script used to generate this numerical example is available for use under an open source licence (4). We note that, although this script (more specifically, the method used to solve (12)) performs well for the numerical example in this paper, it is not

i	$a_{0,i}$	$a_{1,i}$	$a_{2,i}$	$a_{3,i}$	$K_i \times 10^4$	$K_i^* \times 10^4$	F_i
1	0.2121	7.0711	0.1061	3.5355	$\sqrt{2}$	$1/\sqrt{2}$	(0,0,0.1586)
2	0.2121	7.0711	0.1061	3.5355	$\sqrt{2}$	$1/\sqrt{2}$	(0.1760,0,0)
3	0.2121	7.0711	0.1061	3.5355	$\sqrt{2}$	$1/\sqrt{2}$	(0,-0.1954,0)
4	0.2121	7.0711	0.1061	3.5355	$\sqrt{2}$	$1/\sqrt{2}$	(-0.2169,0,0)
5	0.2121	7.0711	0.1061	3.5355	$\sqrt{2}$	$1/\sqrt{2}$	(0,0.2407,0)
6	0.2121	7.0711	0.1061	3.5355	$\sqrt{2}$	$1/\sqrt{2}$	
7	0.2121	7.0711	0.1061	3.5355	$\sqrt{2}$	$1/\sqrt{2}$	
8	0.2121	7.0711	0.1061	3.5355	$\sqrt{2}$	$1/\sqrt{2}$	
9	0.2121	7.0711	0.1061	3.5355	$\sqrt{2}$	$1/\sqrt{2}$	
10	0.2121	7.0711	0.1061	3.5355	$\sqrt{2}$	$1/\sqrt{2}$	
11	0.2121	7.0711	0.1061	3.5355	$\sqrt{2}$	$1/\sqrt{2}$	
12	0.2121	7.0711	0.1061	3.5355	$\sqrt{2}$	$1/\sqrt{2}$	
13			0.1500	5		1	
14			0.1500	5		1	
15			0.1500	5		1	
16			0.1500	5		1	
17			0.1061	3.5355		$1/\sqrt{2}$	
18			0.1061	3.5355		$1/\sqrt{2}$	
19			0.1061	3.5355		$1/\sqrt{2}$	
20			0.1061	3.5355		$1/\sqrt{2}$	
21			0.1061	3.5355		$1/\sqrt{2}$	
22			0.1061	3.5355		$1/\sqrt{2}$	
23			0.1061	3.5355		$1/\sqrt{2}$	
24			0.1061	3.5355		$1/\sqrt{2}$	
25			0.1061	3.5355		$1/\sqrt{2}$	
26			0.1061	3.5355		$1/\sqrt{2}$	
27			0.1061	3.5355		$1/\sqrt{2}$	
28			0.1061	3.5355		$1/\sqrt{2}$	
29			0.15	5		1	
30			0.15	5		1	
31			0.15	5		1	
32			0.15	5		1	
33			0.15	5		1	
34			0.15	5		1	
35			0.15	5		1	
36			0.15	5		1	

TABLE 2 *Given forces on nodes and material properties.*

i	X_i	X_i^*	y_i	$\|y_i\|$	y_i^*	$\|y_i^*\|$
1	(-0.3652,0.4054,1.835)	(-3.5361,0.3588,1.1262)	(6.3418,0.0931,1.4175)	6.4990	(-3.2129,-1.0293,0)	3.3737
2	(5.0234,0.3122,0.4175)	(-0.3232,1.3881,1.1262)	(-0.0839,-1.9656,1.4175)	2.4248	(-2.6523,1.0293,0)	2.8451
3	(-0.2813,-1.5274,0.4175)	(2.3291,0.3588,1.1262)	(-5.3886,0.0931,1.4175)	5.5727	(2.6523,0.9198,0)	2.8073
4	(-6.707,0.3122,0.4175)	(-0.3232,-0.5610,1.1262)	(-0.0839,1.9328,1.4175)	2.3983	(3.2129,-0.9198,0)	3.3419
5	(-0.2813,2.3709,0.4175)	(-3.4941,-0.6076,0.4175)	(6.4257,-1.8396,0)	6.6839	(-0.042,0.9664,0.7087)	1.1992
6	(0,0,-1)	(-3.4941,1.3416,0.4175)	(-6.4257,-2.0587,0)	6.7475	(-0.0420,-0.9828,0.7087)	1.2124
7		(2.3711,1.3416,0.4175)	(-5.3047,2.0587,-0.0000)	5.6901	(3.1709,0.0466,0.7087)	3.2495
8		(2.3711,-0.6076,0.4175)	(5.3047,1.8396,0)	5.6146	(-2.6943,0.0466,0.7087)	2.7863
9		(-3.3535,0.1561,-0.2913)	(6.7070,-0.3122,-1.4175)	6.8623	(-0.042,-0.9828,0.7087)	1.2124
10		(-0.1406,1.1855,-0.2913)	(0.2813,-2.3709,-1.4175)	2.7766	(-0.042,0.9664,0.7087)	1.1992
11		(2.5117,0.1561,-0.2913)	(-5.0234,-0.3122,-1.4175)	5.2289	(-2.6943,0.0466,0.7087)	2.7863
12		(-0.1406,-0.7637,-0.2913)	(0.2813,1.5274,-1.4175)	2.1027	(3.1709,0.0466,0.7087)	3.2495
13					(0,-1.9492,0)	1.9492
14					(-5.8652,0,0)	5.8652
15					(0,1.9492,0)	1.9492
16					(5.8652,0,0)	5.8652
17					(-3.3535,0.1561,0.7087)	3.4311
18					(-0.1406,-0.7637,0.7087)	1.0513
19					(-0.1406,1.1855,0.7087)	1.3883
20					(-3.3535,0.1561,0.7087)	3.4311
21					(2.5117,0.1561,0.7087)	2.6144
22					(-0.1406,1.1855,0.7087)	1.3883
23					(-0.1406,-0.7637,0.7087)	1.0513
24					(2.5117,0.1561,0.7087)	2.6144
25					(-3.2129,-1.0293,0)	3.3737
26					(-2.6523,1.0293,0)	2.8451
27					(2.6523,0.9198,0)	2.8073
28					(3.2129,-0.9198,0)	3.3419
29					(-5.8652,0,0)	5.8652
30					(0,1.9492,0)	1.9492
31					(-5.8652,0,0)	5.8652
32					(0,1.9492,0)	1.9492
33					(-0.1826,0.2027,1.4175)	1.4435
34					(-0.1826,0.2027,1.4175)	1.4435
35					(-0.1826,0.2027,1.4175)	1.4435
36					(-0.1826,0.2027,1.4175)	1.4435

TABLE 3 *Final nodes, edges, and edge lengths.*

optimal for larger networks: as the size of system increases, $\tilde{A}$ becomes more sparse, therefore $\tilde{A}_{11}$, $\tilde{A}_{12}$, B^P, and X^Q should be stored as sparse matrices to speed up MATLAB's '\' function.

Conclusions

In this article we proposed a mathematical model of elasticity with exact kinematics, where the intrinsically discrete structure of materials is represented by two graphs and analysed using calculus on discrete manifolds. By making the kinematics of one of the graphs induced by the kinematics of the other, we derived the governing equations of elasticity where the deformations of both graphs contribute energy to the system, but the reaction of the system is only via forces in the edges of latter graph. This provides a single non-linear system of governing equations, for which we offered linearisation, computational implementation, and a

simple demonstration of the model at work. The numerical example shown is for a particular simple arrangement of neighbours of a single vertex, but the model is applicable to any spatial arrangement of vertices and their connectivity, e.g. an arrangement arising from a Voronoi tessellation of a domain with randomly distributed nodes as described in Section 2. The model requires extensive testing with larger lattices to compare with experimentally measured elastic behaviour of various materials, which is a subject of ongoing work. We anticipate that the model can be used for atomic scale simulations as an alternative to the currently used in molecular dynamics interactions based on empirical pair and cohesive potentials. Our expectation is based on the following observation. The original atomic scale models used only pair potentials, e.g. Lenard-Jones or Morse, suitable for neutral atoms and molecules, and were later complemented by cohesive terms, e.g. in embedded atom and Finnis-Sinclair models, for describing the behaviour of crystalline lattices [new citation]. The latter were still further modified to include angular dependences of the cohesive potentials in order to capture the complex interaction of a single metal atom with its neighbourhood. The calibration of such potential functions is increasingly difficult and involves a great degree of empiricism. Our proposition is that the method described here will allow for capturing the complex linear and angular interactions by the combination of energies stored in the primary and complementary lattices. Testing this proposition is one of the avenues for future work on the model developed here. In addition, we plan to compare the two-graph approach with an approach based on a 3-complex description of solids, which is still under development. It will be important to demonstrate to what extent the two-graph approach is an approximation to the ”exact” 3-complex solution, in order to justify the applicability of the former as computationally more efficient.

Acknowledgments

I. Dassios is supported by Science Foundation Ireland (Strategic Partnership Programme Grant Number SFI/15/SPP/E3125). G. J. O’Keeffe acknowledges the support of the Irish Research Council (GOIPG/2014/887). AP Jivkov acknowledges gratefully the financial support of EPSRC via grant EP/N026136/1 ”Geometric Mechanics of Solids”.

References

[1] G. Cusatis, Z.P. Bazant, L. Cedolin. Confinement-shear lattice CSL model for fracture propagation in concrete. Computer Methods in Applied Mechanics and Engineering 195 (2006) 7154-7171.

[2] I. Dassios, A. Jivkov, A. Abu-Muharib, P. James. A mathematical model for plasticity and damage: A discrete calculus formulation. Journal of Computational and Applied Mathematics, Elsevier, Volume 312, Pages 27-38 (2017). DOI 10.1016/j.cam.2015.08.017.

[3] Dassios I. Stability of basic steady states of networks in bounded domains. Computers & Mathematics with Applications, Elsevier, Volume 70, Issue 9, pp. 2177-2196 (2015).

[4] I. Dassios, G.J. O’Keeffe, A. Jivkov. MATLAB script for example in 2018 paper: A mathematical model for elasticity using calculus on discrete manifolds (Version v1.0). Zenodo, (2018). DOI 10.5281/zenodo.1157967.

[5] Esqueda, H., Herrera, R., Botello, S., & Moreles, M. A. (2018). A geometric description of Discrete Exterior Calculus for general triangulations. arXiv preprint arXiv:1802.01158.

[6] L.J. Grady, J.R. Polimeni. Discrete Calculus: Applied Analysis on Graphs for Computational Science. Springer, London, 2010.

[7] D.V. Griffiths, G.G.W. Mustoe. Modelling of elastic continua using a grillage of structural elements based on discrete element concepts. International Journal for Numerical Methods in Engineering 50 (2001) 1759-1775.

[8] A.P. Jivkov, J.R. Yates. Elastic behaviour of a regular lattice for meso-scale modelling of solids. International Journal of Solids and Structures 49 (2012) 3089-3099.

[9] B.L. Karihaloo,P.F. Shao, Q.Z. Xiao. Lattice modelling of the failure of particle composites. Engineering Fracture Mechanics 70 (2003) 2385-2406.

[10] Y. Wang, P. Mora. Macroscopic elastic properties of regular lattices. Journal of the Mechanics and Physics of Solids 56 (2008) 3459-3474.

[11] A. Yavari. On geometric discretization of elasticity. Journal of Mathematical Physics 49 (2008) 022901.

[12] M. Zhang, C.N. Morrison, A.P. Jivkov. A meso-scale site-bond model for elasticity: Theory and calibration. Materials Research Innovations 18 (2014) S2-982-986.

[13] D. C. Rapaport (1 April 2004). The Art of Molecular Dynamics Simulation. Cambridge University Press.